Supplementary Figures

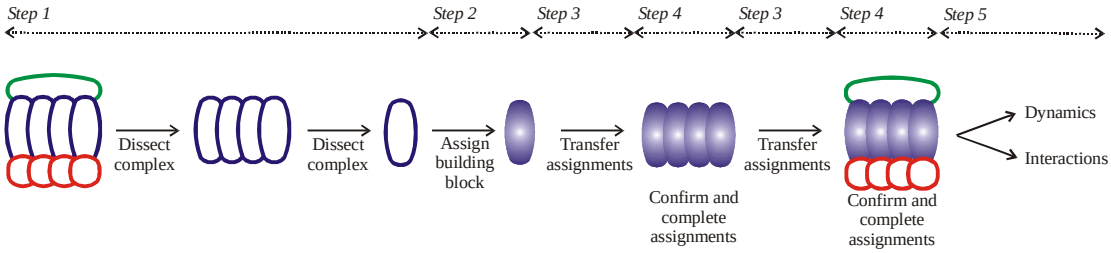

Figure S1: Strategy for the assignment of Ile-δ1, Leu and Val methyl correlations in supra-molecular complexes.

Step 1: Dissect the high molecular weight complex into smaller building blocks such as monomeric proteins or protein domains. This typically requires several iterations of mutagenesis, based to a large extent on the X-ray structure of the supra-molecular complex that provides an indication as to what residues might be important in stabilizing the complex. These smaller units can also be of high molecular weight (purple complex, corresponding to the 360 kDa $\alpha_7\alpha_7$ of the 20S proteasome CP) but typically have improved spectral quality relative to the largest complex (of interest) or can be expressed to higher yield.

Step 2: Assign the smallest building block (the 21 kDa $\alpha_{monomer}$ in the example of the 20S proteasome CP) using standard 'backbone' and 'side-chain' triple resonance multi-dimensional NMR methods[1]. The structures of the smallest building block (and indeed larger complexes) in isolation and in the context of the complete particle should be similar. This can be ascertained by comparing the predicted secondary structure of the smallest building block obtained on the basis of the assigned chemical shifts with the secondary structure observed in crystal structure of the complex and by using NOE spectra to confirm that distances are in keeping with expectations based on the X-ray model.

Step 3: Transfer $^{1}H,^{13}C$ assignments of Ile, Leu and Val methyl groups to larger complexes. In the general case it will not be possible to transfer assignments between two-dimensional $^{1}H,^{13}C$ methyl-TROSY spectra of different molecular species directly since even subtle changes in chemical shifts between spectra can make such a process highly ambiguous. Thus, additional data sets must be recorded. In this regard, high sensitivity methyl-TROSY based spectra that correlate methyl $^{1}H,^{13}C$ chemical shifts with those from the nearest and next nearest ^{13}C spins[2] (for example, Cβ and Cα, respectively, in the case of Val) are valuable. This allows the comparison of methyl *and* side-chain chemical shifts from the smallest building block ($\alpha_{monomer}$) and the next largest complex ($\alpha_7\alpha_7$). In cases where the correspondence is high the methyl assignments can then be transferred from the monomer to the next largest complex. In addition to COSY-based experiments, NOE data sets can be recorded on both monomer ($\alpha_{monomer}$) and oligomer ($\alpha_7\alpha_7$) and patterns of NOEs can be compared to aid the assignment.

Step 4: Transferred assignments are confirmed using NOE correlations and expected distances based on the X-ray coordinates. Additional assignments (that could not be obtained directly in step 3 because chemical shifts between complexes changed significantly) can be made on the basis of observed NOEs. Furthermore, a mutational approach can be used to provide additional assignments. In practice Steps 3 and 4 are iterated to complete the transfer of assignments from the 'isolated' oligomer to the full complex.

Step 5: The obtained assignments for the supra-molecular complex form the basis for all further studies such as measurement of site specific side-chain dynamics and molecular interactions.

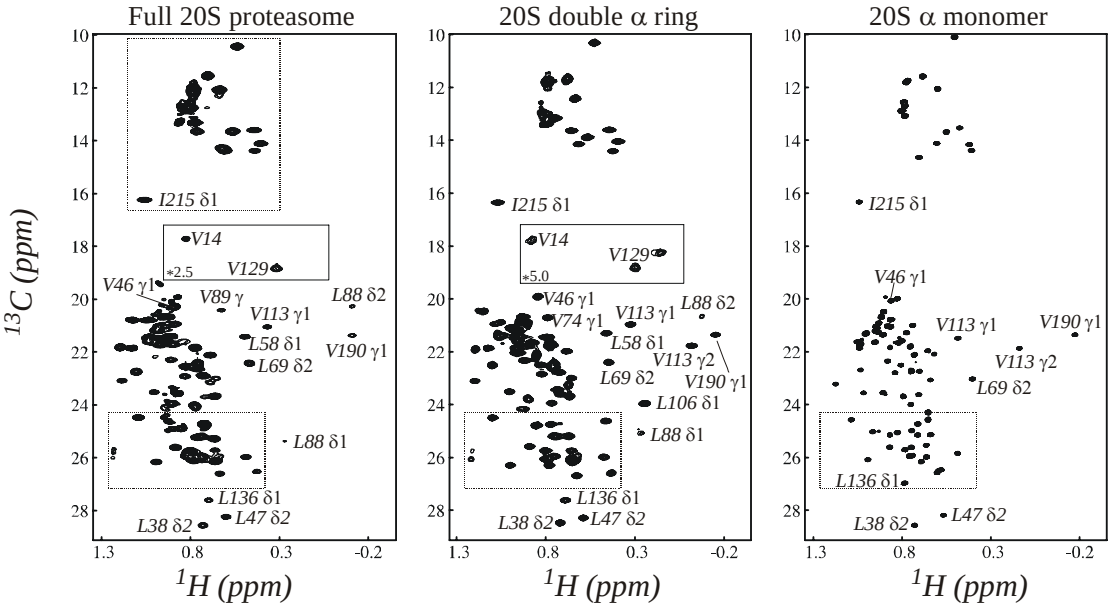

Figure S2: HMQC TROSY spectra of $\alpha_7\beta_7\beta_7\alpha_7$ (CP), $\alpha_7\alpha_7$ and $\alpha_{monomer}$

Spectra of U-[^{2}H,^{12}C], Ileδ1-[$^{13}CH_3$] , Leu,Val-[$^{13}CH_3$,$^{12}CD_3$] labeled proteasome species recorded at 800 MHz (^{1}H frequency) and 65^{o}C (CP) or 50^{o}C ($\alpha_7\alpha_7$, $\alpha_{monomer}$). Assignments for some residues are indicated. The dashed boxes are enlarged in Figures 1b-e. Regions in boxes indicated by continuous lines are plotted at a lower contour level so that weak resonances can be visualized. Note that only the α subunits are NMR active (see Methods). It should be noted that a number of methyl groups in the full CP that are proximal to the α,β interface could not be assigned because their resonances were broadened beyond detection from relaxation contributions arising from the protonated β-rings. Reconstituting the CP with a deuterated version of the β subunits would eliminate this broadening.

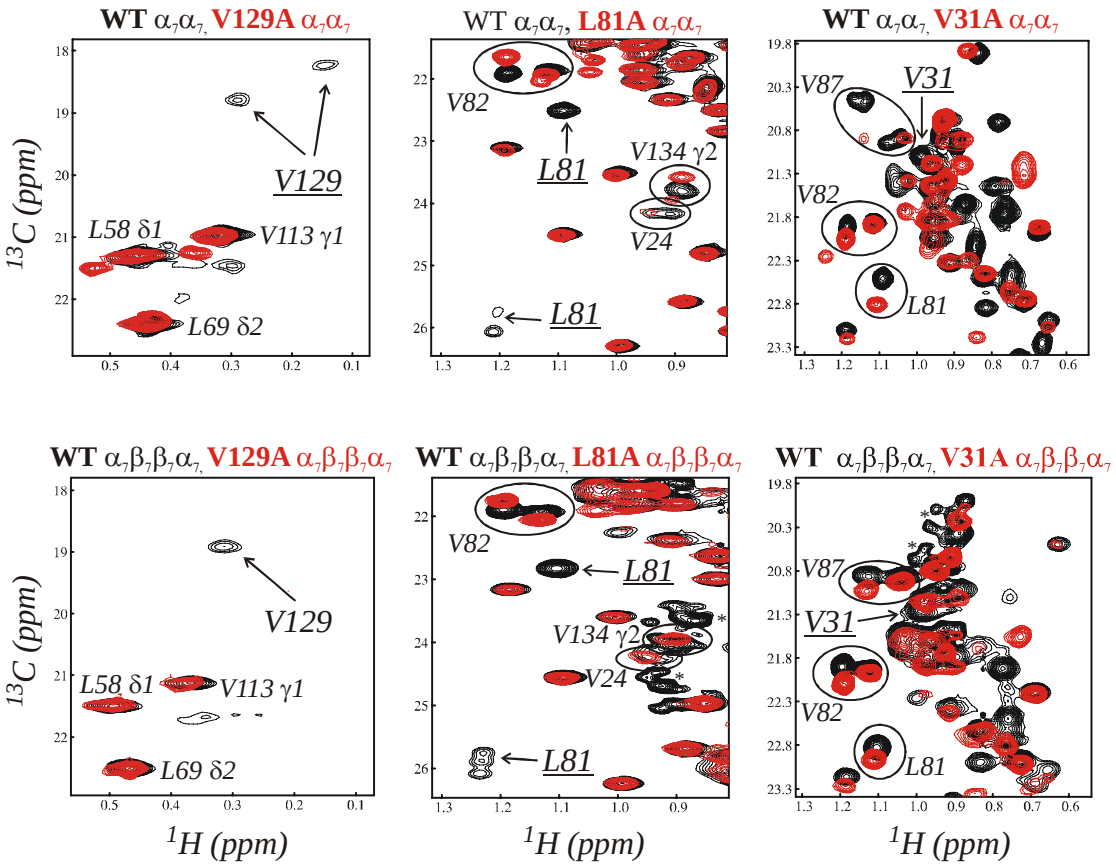

Figure S3: Use of mutations as an aid in assignment

Overlay of spectra of WT (black) and mutant (red, V129A, L81A or V31A) proteins, illustrating the three scenarios that have been observed in using a mutational approach for assignment. Case 1: Effects of the mutation are limited (for example, V129A) allowing a straightforward assignment. Case 2: The mutation causes chemical shift changes of correlations derived from residues in spatial proximity to the site of mutation (L81A). Peaks that change chemical shift due to the mutation are indicated with ovals. These changes can make the assignment more difficult in the absence of additional information. Case 3: Dramatic effects are observed in spectra (V31A), preventing assignment of the mutated residue in the absence of additional information. Assignment of V31 was not possible based on mutational data alone, and was assigned based on NOE spectra. Correlations denoted by * ($\alpha_7\beta_7\beta_7\alpha_7$) are derived from impurities that were not present in all spectra.

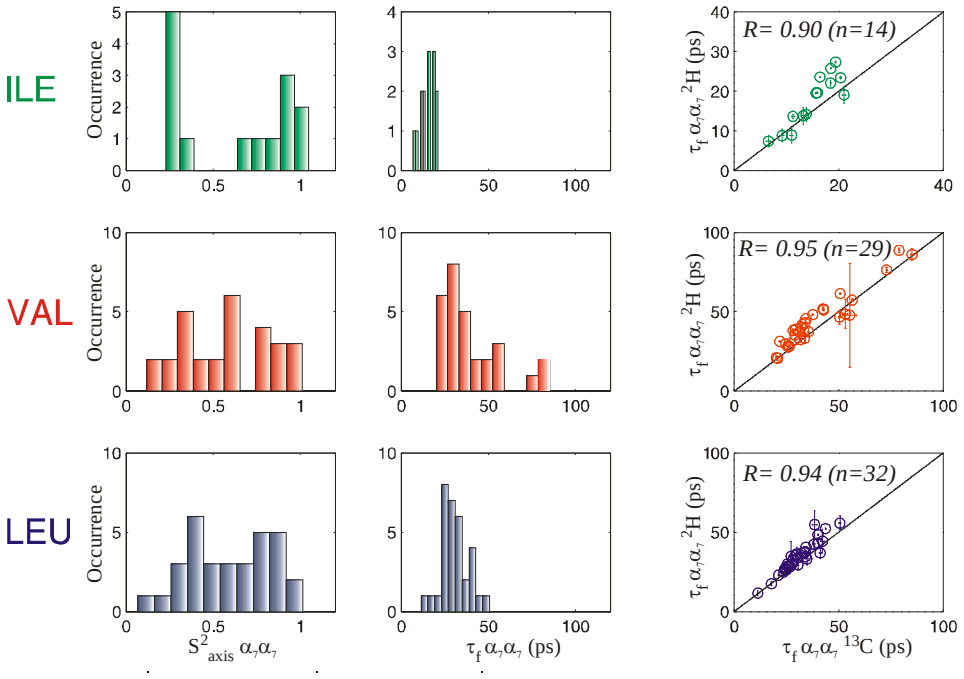

Figure S4: Distribution of S^2 values and internal correlation times as measured for $\alpha_7\alpha_7$

Left: Histograms of S^2 values extracted from carbon T_1 and T_2 relaxation times, measured on a U-[^{2}H],Ile-δ1-[$^{13}CHD_2$], Leu, Val [$^{13}CHD_2$,$^{13}CHD_2$]-labeled $\alpha_7\alpha_7$ sample, 50^{o}C.

Middle: Histograms of values of the correlation time τ_f , sensitive to rotation of and about the methyl three-fold axis[3], derived from carbon relaxation experiments[4].

Right: Correlation between τ_f values obtained from deuterium and carbon relaxation experiments.

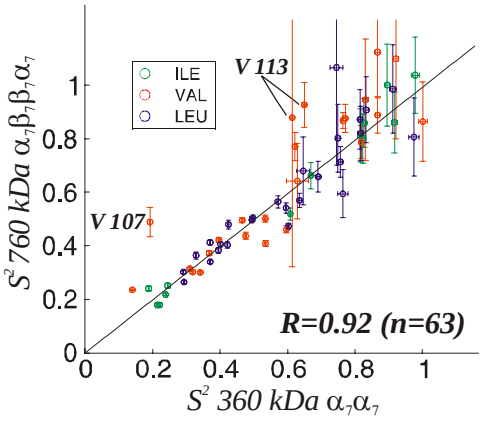

Figure S5: Correlation of fast time-scale dynamics in $\alpha_7\alpha_7$ and the CP

Correlation between S^2 values in the 360 kDa $\alpha_7\alpha_7$ (50°C) and in the 670 kDa full proteasome CP (65°C).

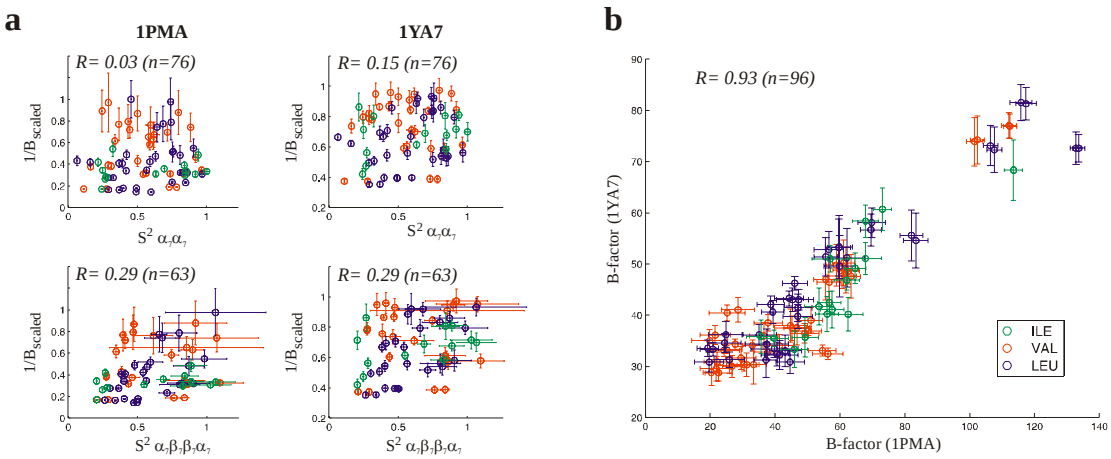

Figure S6: S^2 *vs* crystallographic B-factors

a. Correlation between S^2 and $(1/B)_{scaled}$ (1/B scaled so that the maximum value is 1) for Ile-δ1, Leu-δ and Val-γ methyl groups of $\alpha_7\alpha_7$ (top) and $\alpha_7\beta_7\beta_7\alpha_7$ (bottom). B factors were derived from a pair of crystal structures, 1PMA[5] (left) and 1YA7[6] (right), and the plotted values are averaged over the 14 subunits. b. Correlation between the temperature factors for Ile-δ1, Leu-δ and Val-γ methyl groups of the two independently determined structures, 1PMA and 1YA7.

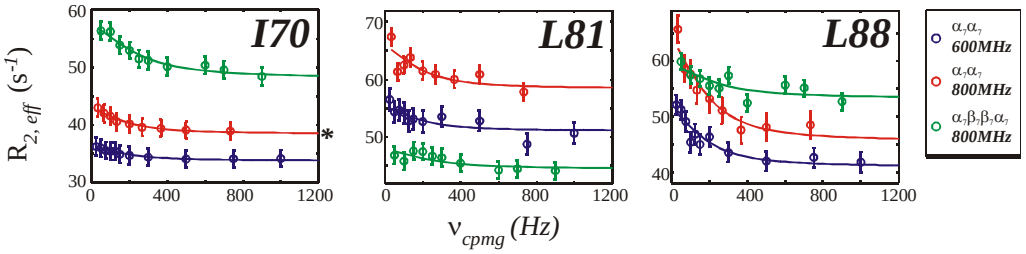

Figure S7: Studies of ms time-scale dynamics

Fits of multiple-quantum methyl-TROSY dispersion profiles[7] based on a single common exchange rate for either $\alpha_7\alpha_7$ (red and blue) or the full proteasome (green). $5s^{-1}$ is added to the profile marked with * to improve the clarity of the figure.

Supplementary information

Sample Preparation:

The *T. acidophilum* α and β proteasome subunits were cloned into modified pET vectors from genomic DNA (American Type Culture Collection, Manassas, VA). The 11S regulator from *Trypanosoma brucei* (PA26) was cloned into a pProEx vector (Invitrogen). Mutations were introduced using the Quikchange (Stratagene) approach. *E.coli* BL21(DE3)-codon plus cells expressing the α proteasome subunit were grown in 99% or 70% D_2O minimal medium containing $^{15}NH_4Cl$ as the sole nitrogen source and [$^{2}H/^{12}C$]- or [$^{2}H/^{13}C$]-glucose as the carbon source. To achieve methyl labelling, the media was supplemented with 60mg/L alpha-ketobutyric acid ([methyl-$^{13}CH_3$] or [methyl-$^{13}CHD_2$]) and 100 mg/L alpha-ketoisovaleric acid ([dimethyl-($^{13}CH_3$)$_2$], [dimethyl-$^{13}CH_3$,$^{12}CD_3$] or [dimethyl-($^{13}CHD_2$)$_2$]) 1 hour prior to protein induction[8]. *E.coli* BL21(DE3)-codon plus cells expressing the unlabelled proteasome subunits or the 11S activator were grown in LB medium. Samples were purified as described in Methods. In the case of samples of $\alpha_{monomer}$, prepared using deuterated media and used to obtain complete backbone or methyl side-chain assignments, back-exchange of amide sites with protons was achieved by an unfolding/refolding protocol that involved extensive dialysis of the guanidine-denatured protein (0.1-0.5 mg/ml) against 100mM sodium phosphate pH 7.8, 150mM KCl and 10% glycerol.

NMR Experiments:

NMR experiments were recorded at 600 MHz (^{1}H resonance frequency; cryogenically cooled probe-head) or 800 MHz (room temperature probe-head). Data sets for

$\alpha_{monomer}$ and $\alpha_7\alpha_7$ were obtained at 50°C, while all spectra measured on the CP ($\alpha_7\beta_7\beta_7\alpha_7$) were recorded at 65°C, 800 MHz.

Experiments recorded on $\alpha_{monomer}$: Chemical shift assignments were obtained using standard 3D TROSY-based triple resonance experiments[9,10] recorded on a 1.6 mM U-[^{2}H,^{15}N,^{13}C]-labeled sample. Each of HNCA, HNCO, HN(CO)CA, HN(CA)CO and HNCACB 3D data set was recorded in approximately 24 hours. Side-chain ^{13}C and ^{1}H chemical shifts were obtained via (H)C(CO)NH-TOCSY and H(C)(CO)NH-TOCSY[11,12] experiments, respectively, recorded in 1.5 days/data set on a U-[70%^{2}H,^{15}N,^{13}C]-labeled sample. An HMQC (^{13}C-t_1)-NOE-HMQC-(^{13}C-t_2,^{1}H-t_3) spectrum of U-[^{2}H],Ile-δ1-[$^{13}CH_3$], Leu, Val [$^{13}CH_3$,$^{12}CD_3$]-labeled $\alpha_{monomer}$ (*i.e.*, only one of the two methyl groups of Leu and Val is $^{13}CH_3$ labeled) was recorded on a 2 mM sample in 88 hours using a mixing time of 250 ms.

Experiments for assignment of $\alpha_7\alpha_7$: Methyl-TROSY out-and-back COSY-based data sets that are based on previously published COSY experiments for the assignment of methyl groups in Ile, Leu and Val side-chains[2] were recorded on a 1.4 mM (monomer concentration) sample of U-[^{2}H,^{13}C],Ile-δ1-[$^{13}CH_3$], Leu, Val [$^{13}CH_3$,$^{12}CD_3$]-labeled $\alpha_7\alpha_7$. A pair of pulse schemes were employed: H_{methyl}-C_{methyl}-$C_{\beta/\gamma}(t_1)$-$C_{methyl}(t_2)$-$H_{methyl}(t_3)$, where correlations of the form ($\omega^{13}C^{\beta}$,$\omega^{13}C^{methyl}$, ω^1H^{methyl}) and ($\omega^{13}C^{\gamma}$,$\omega^{13}C^{methyl}$, ω^1H^{methyl}) are obtained for Val and Ile/Leu residues, respectively, and H_{methyl}-C_{methyl}-($C_{\beta/\gamma}$)-$C_{\alpha/\beta}(t_1)$-($C_{\beta/\gamma}$)-$C_{methyl}(t_2)$-$H_{methyl}(t_3)$ where cross-peaks at ($\omega^{13}C^{\alpha}$,$\omega^{13}C^{methyl}$, ω^1H^{methyl}) and ($\omega^{13}C^{\beta}$,$\omega^{13}C^{methyl}$, ω^1H^{methyl}) are generated for Val and Ile/Leu. Each of the data sets was recorded in approximately 20 hours. A NOESY

spectrum was obtained on a 2 mM U-[^{2}H],Ile-δ1-[$^{13}CH_3$], Leu, Val [$^{13}CH_3$,$^{12}CD_3$]-labeled sample in 90 hours at 800 MHz (250 ms mixing time).

Relaxation experiments on $\alpha_7\alpha_7$*:* ^{13}C T_1 and T_2 data sets[4] were recorded on a 2.8 mM (monomer concentration) U-[^{2}H],Ile-δ1-[$^{13}CHD_2$], Leu, Val [$^{13}CHD_2$,$^{12}CHD_2$]-labeled sample at 600 MHz in 15 hours/data set. ^{2}H T_2 and T_1 experiments[13,14] were obtained on the same sample, 600 MHz, in 60 and 110 hours, respectively, reflecting the 5-fold (T_2) and 13-fold (T_1) decrease in sensitivity relative to the corresponding ^{13}C experiments. Relaxation times were obtained by recording a series of experiments with parametrically varied relaxation delays with maximum durations of 1.8s (^{13}C T_1), 40ms (^{13}C T_2), 45ms (^{2}H T_1) and 1.8ms (^{2}H T_2) and order parameters were extracted as described[4,13]. Values for the ratio of the principal components of the diffusion tensor were estimated from hydrodynamic calculations[15], producing $D_{par}/D_{perp} = 1$. The overall rotational correlation time was adjusted to 120ns so that the extracted order parameters are between 0 and 1. Methyl-TROSY multiple-quantum relaxation dispersion data sets[7] were recorded on a 2 mM U-[^{2}H,^{12}C],Ile-δ1-[$^{13}CH_3$], Leu, Val [$^{13}CH_3$,$^{12}CD_3$]-labeled sample using constant-time relaxation delays of 40 ms (600 MHz, 11 ν_{CPMG} points) and 30 ms (800 MHz, 9 ν_{CPMG} points) and total acquisition times of 30 and 23 hours, respectively.

Experiments for assignment of $\alpha_7\beta_7\beta_7\alpha_7$: NOESY spectra were recorded on 0.6 and 0.4 mM (monomer concentrations) U-[^{2}H],Ile-δ1-[$^{13}CH_3$], Leu, Val [$^{13}CH_3$,$^{12}CD_3$]-labeled (250 ms mixing time) and U-[^{2}H],Ile-δ1-[$^{13}CH_3$], Leu, Val [$^{13}CH_3$,$^{13}CH_3$]-labeled (50 mixing time) samples in 112 hours/data set at 800 MHz.

Relaxation experiments on $\alpha_7\beta_7\beta_7\alpha_7$*:* A methyl-TROSY multiple quantum relaxation dispersion data set was recorded on a 0.6 mM (monomer concentration) U-[^{2}H,^{12}C],Ile-δ1-[$^{13}CH_3$], Leu, Val [$^{13}CH_3$,$^{12}CD_3$]-labeled sample, 800 MHz with a constant-relaxation time delay of 20 ms (800 MHz, 10 ν_{CPMG} points). ^{13}C T_1 and T_2 relaxation times were measured on a 1.8 mM (monomer concentration) U-[^{2}H],Ile-δ1-[$^{13}CHD_2$], Leu, Val [$^{13}CHD_2$,$^{12}CHD_2$]-labeled sample at 800 MHz in 24 and 130 hours, respectively. A series of data sets were recorded with maximum relaxation delays up to 2.0s (^{13}C T_1) and 25ms (^{13}C T_2). D_{par}/D_{perp} was calculated[15] to be 1.5 and used throughout the analysis, along with an overall correlation time of 180 ns that ensures that order parameters are between 0 and 1.

Measurement of αα/11S and αββα/11S binding constants:

Consider the following sequential ligand dissociation processes,

$$PL \rightleftarrows P+L\ ,\ K_{D,1}=(K_D/2)=[P][L]/[PL] \qquad \text{(S1)}$$

$$PL_2 \rightleftarrows PL+L\ ,\ K_{D,2}=2K_D=[PL][L]/[PL_2] \qquad \text{(S2)}$$

where [P]=[$\alpha_7\alpha_7$], [L]=[11S], [PL]=[11S-$\alpha_7\alpha_7$]+[$\alpha_7\alpha_7$-11S], [PL_2]=[11S-$\alpha_7\alpha_7$-11S] and 11S-$\alpha_7\alpha_7$, $\alpha_7\alpha_7$-11S and 11S-$\alpha_7\alpha_7$-11S correspond to binding to the 'first', 'second' and both rings, respectively. Here we have assumed that each binding step is equivalent (*i.e.*, the microscopic dissociation constants are the same). In the notation used we have also assumed that 11S is titrated into a solution of $\alpha_7\alpha_7$; in the case that the titration involves a solution of the CP, $\alpha_7\alpha_7$ is replaced by $\alpha_7\beta_7\beta_7\alpha_7$. From eqs. S1 and S2 we can write

$$[P_{free}]=[P_{total}]/(1+K_D^{-1}[L_{free}])^2,$$

$$[PL]=[P_{total}]-[PL_2]-[P_{free}], \quad \text{(S3)}$$

$$[PL_2]=K_D^{-2}[P_{free}][L_{free}]^2$$

where $[P_{free}]$ and $[P_{total}]$ are the concentrations of the free and total protein, respectively and the free ligand concentration $[L_{free}]$ is obtained from the relationship

$$[L_{free}]=\frac{-b+\sqrt{b^2+4K_D^{-1}[L_{total}]}}{2K_D^{-1}}, \quad \text{(S4)}$$

where $[L_{total}]$ is the total ligand concentration and $b=1+2K_D^{-1}[P_{total}]-K_D^{-1}[L_{total}]$. In the limit where (i) there is no change in the intensity of correlations from the exchange process (very slow exchange), (ii) all species of protein in solution have the same intrinsic transverse relaxation rates, and (iii) the chemical shifts from one binding site on the protein are independent of the ligation state of the other site, the intensities of correlations derived from free and bound forms of protein are given by (neglecting a scaling factor)

$$I_{free} = (2[P_{free}]+[PL])/(2[P_{total}]), \quad \text{(S5.1)}$$

$$I_{bound} = (2[PL_2]+[PL])/(2[P_{total}]) \quad \text{(S5.2)}$$

where $[P_{free}]$, $[PL]$ and $[PL_2]$ can be expressed in terms of $[L_{total}]$ and $[P_{total}]$ using eqs S3 and S4 above.

When the titration data is fit on a per-residue basis to equations of the form described by S5.1 and S5.2 an average K_D value of 8 μM is obtained with a standard deviation of 6 μM; all the data fitted together produce a K_D of 8 μM. This analysis is strictly speaking valid only in the limit that exchange contributions to intensities of

correlations can be neglected and in practice this is unlikely to be the case except for very strong binding. In an effort to establish what sort of errors are associated with the simplified analysis described above we have considered the effects of exchange and relaxation during the HMQC pulse scheme, $90^o(^1H)$-τ-$90^o(^{13}C)$-$t_1/2$-$180^o(^1H)$-$t_1/2$-$90(^{13}C)$-τ-Acq(t_2,^{13}C decoupling), that is used to generate the correlation data. This is done by solving the Bloch-McConnell equations[16] for a description of evolution in each of the intervals in the pulse scheme above that includes intrinsic transverse relaxation for each methyl probe attached to the interconverting species, P, PL and PL_2. An analysis of this sort (using approximate relaxation rates), and fitting cross peak intensities from 19 free and 23 bound correlations simultaneously gives an average K_D value of 12±10μM, Figure 4d, very similar to that obtained by neglecting exchange.

Supplementary References

1. Cavanagh, J., Fairbrother, W., Palmer, A. & Skelton, N. *Protein NMR Spectroscopy: Principles and Practice* (Academic Press, San Diego, 1996).
2. Tugarinov, V. & Kay, L. E. Ile, Leu, and Val methyl assignments of the 723-residue malate synthase G using a new labeling strategy and novel NMR methods. *J Am Chem Soc* **125**, 13868-78 (2003).
3. Kay, L. E., Muhandiram, D. R., Farrow, N. A., Aubin, Y. & Forman-Kay, J. D. Correlation between dynamics and high affinity binding in an SH2 domain interaction. *Biochemistry* **35**, 361-8 (1996).
4. Tugarinov, V. & Kay, L. E. Quantitative 13C and 2H NMR relaxation studies of the 723-residue enzyme malate synthase G reveal a dynamic binding interface. *Biochemistry* **44**, 15970-7 (2005).
5. Lowe, J. et al. Crystal structure of the 20S proteasome from the archaeon T. acidophilum at 3.4 A resolution. *Science* **268**, 533-9 (1995).
6. Forster, A., Masters, E. I., Whitby, F. G., Robinson, H. & Hill, C. P. The 1.9 A structure of a proteasome-11S activator complex and implications for proteasome-PAN/PA700 interactions. *Mol Cell* **18**, 589-99 (2005).
7. Korzhnev, D. M., Kloiber, K., Kanelis, V., Tugarinov, V. & Kay, L. E. Probing slow dynamics in high molecular weight proteins by methyl-TROSY NMR spectroscopy: application to a 723-residue enzyme. *J Am Chem Soc* **126**, 3964-73 (2004).
8. Tugarinov, V., Hwang, P. M. & Kay, L. E. Nuclear magnetic resonance spectroscopy of high-molecular-weight proteins. *Annu Rev Biochem* **73**, 107-46 (2004).
9. Salzmann, M., Pervushin, K., Wider, G., Senn, H. & Wuthrich, K. TROSY in triple-resonance experiments: new perspectives for sequential NMR assignment of large proteins. *Proc Natl Acad Sci U S A* **95**, 13585-90 (1998).
10. Yang, D. W. & Kay, L. E. TROSY triple-resonance four-dimensional NMR spectroscopy of a 46 ns tumbling protein. *J Am Chem Soc* **121**, 2571-5 (1999).
11. Montelione, G. T., Lyons, B. A., Emerson, S. D. & Tashiro, M. An efficient triple resonance experiment using carbon-13 isotropic mixing for determining sequence-specific resonance assignments of isotopically-enriched proteins. *J Am Chem Soc* **114**, 10974-5 (1992).
12. Grzesiek, S., Anglister, J. & Bax, A. Correlation of Backbone Amide and Aliphatic Side-Chain Resonances in 13C/15N-Enriched Proteins by Isotropic Mixing of 13C Magnetization. *J Magn Reson. B* **101**, 114-9 (1993).
13. Tugarinov, V., Ollerenshaw, J. E. & Kay, L. E. Probing side-chain dynamics in high molecular weight proteins by deuterium NMR spin relaxation: an application to an 82-kDa enzyme. *J Am Chem Soc* **127**, 8214-25 (2005).
14. Tugarinov, V. & Kay, L. E. A 2H NMR relaxation experiment for the measurement of the time scale of methyl side-chain dynamics in large proteins. *J Am Chem Soc* **128**, 12484-9 (2006).
15. Garcia de la Torre, J., Huertas, M. L. & Carrasco, B. HYDRONMR: prediction of NMR relaxation of globular proteins from atomic-level structures and hydrodynamic calculations. *J Magn Reson* **147**, 138-46 (2000).
16. McConnel, H. Reaction Rates by Nuclear Magnetic Resonance. *J.Chem.Phys* **28**, 430-1 (1958).